JOURNAL OF PROPULSION AND POWER
Vol. 14, No. 2, March–April 1998

Wake Decay: Effect of Freestream Swirl

J. M. Brookfield,* I. A. Waitz,† and J. Sell*
Massachusetts Institute of Technology, Cambridge, Massachusetts 02139

A study of the effects of freestream swirl on the decay characteristics of wakes shed from a rotating blade row is presented. The freestream swirl behind the rotor causes the wakes to skew tangentially, stretching the wakes as they are convected from the rotor to the stator. The effect of stretching on wake decay is illustrated using a simplified two-dimensional model. The model is described and the results are compared to 1) measurements from a two-dimensional cascade facility where no stretching or skewing of the wakes occurs; 2) solutions obtained using a three-dimensional, Reynolds-averaged Navier–Stokes solver; and 3) experimental wake measurements taken behind a low hub-to-tip ratio fan. For typical fan geometries with hub-to-tip ratios of approximately 0.5 and rotor–stator spacings of one to two rotor chord lengths, the wake can be stretched by over 50%. The stretching increases the mixing rate, which leads to a reduction in the mean wake velocity deficit of approximately 30% and a widening of the wake of about 15%. These effects account for much of the difference seen between cascade wake measurements and those taken behind rotating fan blade rows. It is therefore important to include the effects of stretching when using cascade data for prediction of fluid mechanic, acoustic, or structural phenomena associated with fan wakes. Finally, the study also suggests a potential for small (<3 dB) reductions in tonal noise because of wake–stator interaction through tailoring the fan loading distribution to produce particular spanwise wake decay characteristics.

Nomenclature

A = amplitude of wake harmonic
C_p = coefficient of pressure, $(P_e - P_i)/0.5\rho U^2$
L = length of wake in an axial plane
$\mathcal{L}$ = Eqs. (3) and (4)
M = Mach number
P = static pressure
r = radius
t = time
U = fan inlet velocity
u = velocity in x direction in wake relative frame
V = freestream velocity in absolute frame
v = velocity in y direction in wake relative frame
w = velocity in main flow direction, normal to wake relative frame
x = coordinate along wake centerline in wake relative frame
y = coordinate normal to wake centerline in wake relative frame
z = coordinate in main flow direction, normal to wake relative frame
ε = strain rate, $[L(t + \Delta t) - L(t)]/[\Delta t L(t)]$
ζ = wake skew angle, the angle between the radial direction and a projection of a wake vortex line onto an axial plane
θ = angular position or momentum thickness, $\int_{-\infty}^{+\infty} [w(y)/w_{fs}]\{1 - [w(y)/w_{fs}]\}\, dy$
ν = effective viscosity (turbulent)
Ω = rotor angular velocity

Subscripts
e = exit
fs = freestream
i = inlet
s = caused by strain
t = tip
te = blade trailing edge
w = wake

Superscript
$'$ = wake mixing induced

I. Introduction

UNDERSTANDING the behavior of wakes in turbomachinery is important for determining overall performance, including efficiency and pressure rise, as well as for estimating noise, heat transfer, and forced aeroelastic response. In high-bypass-ratio turbomachines the interaction of fan blade wakes with the downstream stator blades is an important noise source, and this is the primary motivation for the wake studies reported in this paper. Although engine noise associated with wake–stator interaction has been reduced through evolutionary changes over the last several decades, it is expected that classical noise mitigation techniques will be insufficient in meeting the NASA Advanced Subsonic Technology Program goal of 6 dB additional reduction in engine noise for next-generation high-bypass turbofans. To achieve this noise reduction goal, a clearer understanding of the flowfield downstream from the fan rotor must be developed.

The objective of this paper is to describe the effect of freestream swirl on the decay of turbomachinery blade wakes. The freestream swirl produced from a loaded, rotating blade row causes the wakes shed from the blades to be stretched and wrapped around the annulus as the wakes are convected downstream. As a result, the relative orientation of the wakes with respect to the downstream stator blades, as well as the wake velocity deficit and width, are changed. It will be shown that the magnitude of the changes in the wake velocity deficit and width are significant and in general depend on the degree of stretching applied to the wake.

A simplified computational model was developed to illustrate these effects. This two-dimensional model allows for stretching of the wake along the wake centerline; factors such as secondary flow and radial wake transport are neglected to show the impact of stretching more clearly. In this paper, the model is described and the results are compared to 1) data

Received May 2, 1997; revision received Sept. 2, 1997; accepted for publication Sept. 18, 1997.

*Graduate Student, Aero-Environmental Research Laboratory.
†Associate Professor of Aeronautics and Astronautics, Aero-Environmental Research Laboratory. Senior Member AIAA.

from a two-dimensional cascade facility where no stretching or skewing of the wakes occurs; 2) solutions obtained using a three-dimensional, unstructured mesh, Reynolds-averaged, Navier–Stokes code; and 3) experimental wake measurements taken on a fan stage. The modeling and experiments were carried out on a $M = 0.8$ tip-speed, low hub-to-tip ratio fan geometry typical of next-generation gas turbine applications.

In Sec. II, the characteristics of rotor wakes are described and previous work on rotor wake behavior and modeling is briefly outlined. Section III describes the analytical and experimental tools used in this investigation. In Sec. IV, the results of the investigation are presented, including comparison of the simplified numerical model to experimental data and discussion of the parametric dependence of wake decay on strain rate. Implications for blade design are also discussed with regard to possible influences on fan wake decay for noise reduction. A summary and conclusions are provided in Sec. V.

II. Characteristics of Rotor Wakes

A. Previous Research

Wakes shed from high-speed rotors can be significantly different from those shed from isolated two-dimensional airfoils. Three-dimensional wake structure in turbomachines is determined by spanwise variations in boundary-layer loading and is influenced to a large extent by unsteady vortex shedding, local boundary-layer separation, and diffuser-like instabilities.[1] As a result of these effects, blade-to-blade variations in wake profiles can be as large as ±100% of the mean wake velocity deficit, and only part of these variations can be attributed to geometrical differences between the individual blades. Further, it has been shown by many researchers that significant radial transport often occurs in the wake. Overall, fairly extensive computations and measurements have been made of both mean and unsteady velocity and pressure profiles downstream from rotating blade rows.[2–5] These results illustrate the complex structure of turbomachinery wakes.

However, despite the many detailed investigations that have been presented, analytical wake mixing models and empirical curve fits used for noise estimation[6,7] are typically based on two-dimensional considerations of wake decay and only predict wake profiles to within 20% in deficit and/or width. Because acoustic waves produced by the interaction of the wake structure with the stationary stator blades are driven by the spatial harmonics of the wakes, these errors would correspond to approximately 2-dB errors in noise prediction for the first few blade passing harmonics. Therefore, additional understanding of the underlying physics that determine three-dimensional wake decay is needed to improve predictions of noise from wake–stator interaction.

B. Kinematics of Wake Skewing

The freestream swirl downstream from a rotating blade row causes the blade wakes to be skewed tangentially and stretched. The resulting orientation of the wake with respect to the downstream stator row influences the spatial harmonic amplitudes of the wake when decomposed in the tangential and radial directions. Skewing thus affects the coupling of pressure fluctuations associated with wake–stator interaction to the three-dimensional acoustic modes and, as a result, can either increase or decrease the radiated noise. These effects are fairly well known. However, the effect that the stretching, which accompanies the wake skewing, has on the mixing and decay of the wake is less well understood. This phenomenon, which can also impact the radiated noise, is the primary focus of this paper.

In this section we describe the kinematics of the wake and derive expressions that relate the skewing and stretching of the wake to the velocity field downstream from the rotor. We will consider a wake vortex line or material element that is shed from the rotor blade trailing edge as it is convected downstream by the mean flow. As the wake element is convected

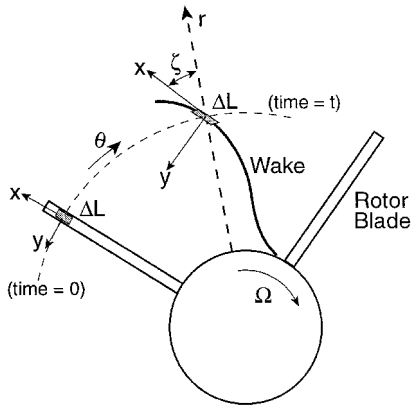

Fig. 1 Position of the wake in an axial plane downstream from the rotor blade trailing edge. (x, y: wake relative reference frame).

downstream, it becomes skewed relative to the radial direction as a result of the swirl in the flow. This is shown schematically in Fig. 1. The skew angle of the wake $\boldsymbol{\zeta}$ relative to the radial direction is related to the increase in length of a wake element as a function of distance downstream. The length of a small wake element projected onto an axial plane at a downstream position z is given approximately by

$$\Delta L(z) = \sqrt{(\mathrm{d}r)^2 + \left[\left(\frac{\partial \theta_w}{\partial r}\right) r\ \mathrm{d}r\right]^2} \tag{1}$$

where θ_w is the angular position of the wake centerline. The angular distance traveled circumferentially in time t by the wake centerline is $\Delta\theta_w(z) = (V_\theta/r)t$, resulting in $\theta_w(z) = \theta_{te} + (V_\theta/r)t$. We assume that radial transport effects are small to more clearly illustrate the effects of stretching (this assumption will be discussed in greater detail in Sec. III.A). The partial derivative of θ_w with respect to r for small initial wake skew angles $\boldsymbol{\zeta}_{te}$ is

$$\frac{\partial \theta_w}{\partial r} = \frac{\tan \zeta_{te}}{r} - t\left(\frac{V_\theta}{r}\right)\left[\frac{1}{r} - \left(\frac{1}{V_\theta}\right)\left(\frac{\mathrm{d}V_\theta}{\mathrm{d}r}\right)\right] \tag{2}$$

Time is given by $t = z/V_z$, thus, the wake element length is

$$\Delta L(z) = \mathrm{d}r\ \sqrt{1 + \left\{\tan \zeta_{te} - z\left(\frac{V_\theta}{V_z}\right)\left[\frac{1}{r} - \left(\frac{1}{V_\theta}\right)\left(\frac{\mathrm{d}V_\theta}{\mathrm{d}r}\right)\right]\right\}^2} \tag{3}$$

which we will later find convenient to write as $\Delta L = \mathcal{L}\ \mathrm{d}r$.

Observing that the wake skew angle is given approximately by $\zeta(z) = \cos^{-1}[\mathrm{d}r/\Delta L(z)]$, the wake skew angle as a function of downstream distance is then given by

$$\zeta(r, z) = \cos^{-1}\left(1 \Big/ \sqrt{1 + \left\{\tan \boldsymbol{\zeta}_{te} - z\left(\frac{V_\theta}{V_z}\right)\left[\frac{1}{r} - \left(\frac{1}{V_\theta}\right)\left(\frac{\mathrm{d}V_\theta}{\mathrm{d}r}\right)\right]\right\}^2}\ \right) = \cos^{-1}(1/\mathcal{L}) \tag{4}$$

Further, to satisfy radial equilibrium for an incompressible flow with 1) a uniform, nonswirling flow entering the rotor, 2) isentropic flow through the rotor, and 3) no axial pressure gradient downstream from the blade row, gradients in the free-

stream tangential velocity are related to gradients in axial velocity by

$$V_z \frac{\mathrm{d}V_z}{\mathrm{d}r} = \left(\Omega - \frac{V_\theta}{r}\right) \frac{\mathrm{d}(rV_\theta)}{\mathrm{d}r} \tag{5}$$

The axial velocity is constant for a free vortex flow where $V_\theta \sim 1/r$. Note that Eq. (5) can be modified to account for more general inlet conditions and nonisentropic rotor flow if required.[8] Using Eqs. (4) and (5), the skew angle of a wake element downstream from the blade row can now be determined as a function of r and z. Equations (3) and (5) can be used to determine the local change in wake length and thus the local strain rate that will be used in the analyses presented in Sec. III.A.

In Eqs. (3) and (4), the influence of the freestream swirl is represented by the two terms in the square brackets. The magnitude of the first term is set largely by the hub-to-tip ratio of the rotor. The second term represents the influence of radial gradients in the tangential velocity field. Depending on the hub-to-tip ratio and the spanwise loading distribution, either term can be dominant, but in typical fan geometries they are of comparable magnitude.

1. Wake Skewing for Simplified Core Compressor and Fan Stages

To illustrate the behavior of wakes in typical turbomachine situations, we consider the simplified case where the rotor has been designed to provide constant work along the span. For an incompressible flow with uniform, nonswirling inlet conditions, this design strategy results in a free vortex flowfield where the tangential velocity varies linearly with radius, such that $V_\theta(r) = V_{\theta t}(r_t/r)$. The downstream tangential velocity is higher at the hub, decreasing monotonically toward the tip. This causes a radial fluid line to skew as it convects downstream because the hub fluid traverses a longer arc length in the period of time required to reach a given downstream location. For this case, the expression for the skew angle of a wake element as a function of radius and downstream distance is

$$\zeta(r, z) = \cos^{-1}\left\{1 \Big/ \sqrt{1 + \left[\tan \zeta_{te} - \left(\frac{2z}{r}\right)\left(\frac{V_\theta}{V_z}\right)\right]^2}\right\} \tag{6}$$

Equation (6) can be used to determine the conditions for which skewing of the wake is important. For a core compressor, a typical hub-to-tip ratio is 0.8, and a typical rotor–stator spacing is 0.4 rotor chords (approximately 3% of the tip radius). Thus, assuming $\zeta_{te} = 0$ and $V_\theta/V_z = 1.0$ at the hub, the wake skew angle is only about 3 deg at the stator location, resulting in little stretching of the wake. Plots of the wake orientation with downstream distance for this case are shown in Fig. 2a. For a typical fan geometry, however, the hub-to-tip ratio is 0.5 and the rotor–stator spacing is greater than 1.5 fan chords (about 30% of the tip radius). The resulting wake skew angle at the inlet to the stator is approximately 30 deg, and the wake is stretched 15%. The stretching increases to 38% at 2.5 chords downstream. Plots of wake orientation for a free vortex fan flow are shown in Fig. 2b. Thus, in low hub-to-tip ratio machines with large rotor–stator axial spacing, significant skewing of the wake is possible. In Sec. IV, the effects that the stretching associated with this wake skew has on the mixing of the wakes will be presented.

2. Effects of Radial Gradients in Axial Velocity

In general, fan and core compressor stages vary somewhat from free vortex designs. Then, as shown in Eq. (5), radial gradients in both axial and tangential velocity are present downstream from the blade row, and the behavior of the wake becomes more complicated to describe. Radial gradients in axial velocity result in portions of the wake being transported more quickly to the stator location, allowing relatively less time for the wake to skew and mix. Thus, wake elements measured at different spanwise locations, in a given axial plane, have been shed from the blade at different times. As a result, the projection onto an axial plane of a wake vortex line, which is shed from the blade at a particular time, is in general different from the intersection that the wake makes with that axial plane when the wake passes through it (the intersection is composed of many different vortex lines shed at different times). It is the wake angle associated with the first of these, the projection of a wake vortex line onto the axial plane [given by Eq. (4)], that is relevant for determining the effect of stretching on wake evolution. Changes in the length of this projection are directly related to changes in the x component of vorticity. It is the increase of this component of vorticity, and the associated shear, that lead to the increase in wake mixing.

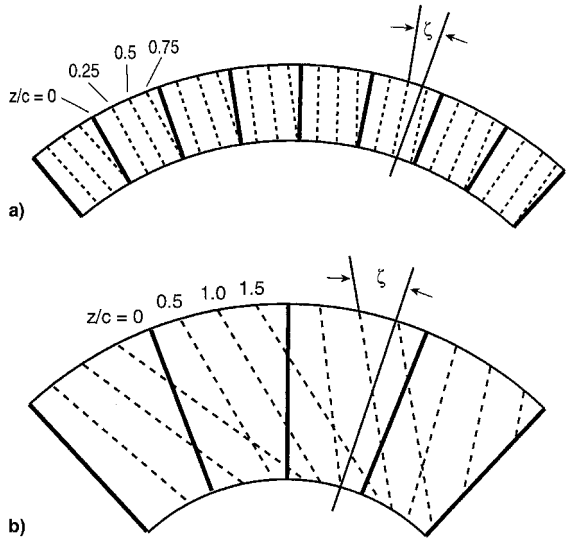

Fig. 2 a) Wake evolution downstream from a core compressor rotor: wake centerline convection at distances downstream corresponding to z/c = 0.25, 0.5, and 0.75. b) Wake evolution downstream from a fan rotor: wake centerline convection at distances downstream corresponding to z/c = 0.5, 1.0, and 1.5.

To illustrate the effects of radial gradients in axial velocity, a radial equilibrium flow with uniform tangential velocity was examined. For this case, the axial velocity as given by Eq. (5) increases by approximately 27% from the hub to the tip. The vortex lines in the wake are skewed relative to the radial direction at an angle of approximately 16 deg at 1.5 chords, as given by Eq. (4). However, because of the radial gradient in axial velocity, the wake intersects an axial plane later at the hub than at the tip. As a result, the intersection of the wake and the axial plane at 1.5 chords is inclined only 4.5 deg from the radial direction. Thus, for cases with radial gradients in axial velocity, the angle associated with the intersection of the wake with an axial plane is not a good estimate of the orientation of the vortex lines in the wake, even for relatively small variations in axial velocity. In general, therefore, axial plane flowfield contours from Navier–Stokes simulations and experimental measurements will not provide relevant wake skew angles for the prediction of wake evolution.

III. Numerical and Experimental Methods

As discussed in the previous section, wakes downstream from fan rotors are typically skewed relative to the radial direction. This skewing stretches the wake and results in an increase in the length of the wake. A simplified numerical model was developed to study the effect of this stretching on the decay of wakes. The development of the model is described in Section III.A. In Sec. IV, the results of the model are compared to results from two-dimensional cascade tests where no

skewing or stretching of the wake occurred, to experimental measurements from a rig test of a low hub-to-tip ratio fan, and to results from a three-dimensional, Reynolds-averaged Navier–Stokes solver. The experimental facilities for the cascade tests and the fan rig tests are described in Sec. III.B and III.C, respectively. The Navier–Stokes solver is discussed in Sec. III.D.

A. Simplified Numerical Model

The wake was assumed to be steady, incompressible, and uniform along its centerline. The assumption of incompressibility is valid even for supersonic fan tip speeds because the convective Mach number (as defined in Ref. 9) of the wake shear layers is typically less than 0.3 for most regions of interest downstream from the rotor. The computational domain is shown in Fig. 3 in the wake relative frame, as defined in Fig. 1. The x axis corresponds to the wake centerline, y is the axis normal to the wake centerline in an axial plane, and z is the freestream flow direction, which would be out of the image in Fig. 3a. The effects of stretching on wake decay were parameterized as a function of the local strain rate, as is typical in mixing problems.[10]

The local strain rate ε is given by the expression $\varepsilon = (1/\Delta L)[\partial(\Delta L)/\partial t] = (V_z/\Delta L)[\partial(\Delta L)/\partial z]$. Taking the partial derivative of the wake element length ΔL, with respect to z, and rewriting Eq. (3) as $\Delta L = \mathcal{L}\, dr$, then

$$\frac{\partial(\Delta L)}{\partial z} = -dr\left(\frac{V_\theta}{V_z}\right)\left[\frac{\sqrt{(\mathcal{L}^2-1)}}{\mathcal{L}}\right]\left[\frac{1}{r}-\left(\frac{1}{V_\theta}\right)\left(\frac{dV_\theta}{dr}\right)\right] \tag{7}$$

Using this expression in the relation for the strain rate provides the local wake strain rate as a function of downstream distance z, and the radial position

$$\varepsilon(r,z) = -V_\theta\left[\frac{\sqrt{(\mathcal{L}^2-1)}}{\mathcal{L}^2(r,z)}\right]\left[\frac{1}{r}-\left(\frac{1}{V_\theta}\right)\left(\frac{dV_\theta}{dr}\right)\right] \tag{8}$$

In the simplified numerical model, the velocities in the x, y, and z directions, respectively, are u, v, and w. Stretching of the wake was prescribed by imposing a velocity $u_s = \varepsilon x$ for uniform strain rate ε, in the x direction. Continuity of mass dictates that the stretch velocity is balanced by $v_s = -\varepsilon y$ to maintain zero axial pressure gradient. The velocities in the x and y directions are then given by $u = u_s + u'$ and $v = v_s + v'$, respectively, where u' and v' are the velocities induced by wake mixing, and u' is assumed to be zero. Assuming derivatives in x and z are much smaller than derivatives in y, the equations for continuity of mass and y and z momentum are written as

$$\frac{\partial(u_s+u')}{\partial x}+\frac{\partial(v_s+v')}{\partial y}+\frac{\partial w}{\partial z}=0 \tag{9a}$$

$$w\frac{\partial v}{\partial z}+v\frac{\partial v}{\partial y}=\nu\frac{\partial^2 v}{\partial y^2} \tag{9b}$$

$$w\frac{\partial w}{\partial z}+v\frac{\partial w}{\partial y}=\nu\frac{\partial^2 w}{\partial y^2} \tag{9c}$$

Note that the stretch-induced velocities, u_s and v_s, will cancel from the mass continuity equation, such that only the entrainment or mixing-induced velocity v' appears in the y direction, giving

$$\frac{\partial v'}{\partial y}+\frac{\partial w}{\partial z}=0$$

In the analysis, it was assumed that the effect of axial pressure gradients on the wake is negligible and that radial velocities are small. Analyses based on Hill et al.[11] can be used to show that the first of these assumptions is good for duct area changes of less than 2%, which are typical of many fan duct designs. For these situations, the change in wake centerline velocity because of the pressure gradient is expected to be less than 3%. The validity of the second assumption, that of small radial velocities, is more difficult to evaluate. In the experiments and numerical simulations presented in Sec. IV, outward velocities along the wake axis (the x direction in the wake-relative frame) of approximately 10% of the freestream velocity magnitude were found. Such velocities would result in a relatively small redistribution of wake fluid (movement on the order of 7% of span by the time the wake reaches the stator location). However, it is also expected that radial wake transport will increase the rate of turbulent exchange in the wake. Indeed, there was a difference in effective viscosity apparent between the cascade experiments and the rig tests presented in Sec. IV. This difference scales approximately with the increase in mean shear found by adding the radial velocity measured in the rig tests to the two-dimensional wake velocity profile measured in the cascade. Such an approximation for the effective viscosity might be applied to take account of the increased turbulent exchange associated with radial transport if the simplified model were to be used to predict wake evolution without a priori knowledge of the flowfield.

The system of equations was solved using centered finite difference methods. Validation of the method and comparisons to experimental results are presented in Sec. IV.

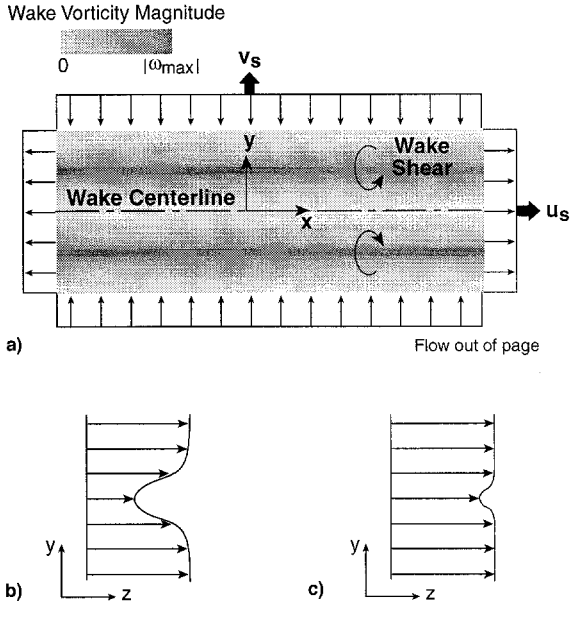

Fig. 3 Effects of stretching on the wake profile: a) induced velocities in the wake relative reference frame, and b) unstretched and c) stretched wake velocity profiles.

B. Cascade Facility

A low-speed ($M \approx 0.03$) cascade facility was used to provide reference data for two-dimensional blade wakes without the influence of stretching. The midspan airfoil from the fan stage used in the rig testing (described in Sec. III.C) was used to produce the wakes. The stage is representative of a next-generation high-bypass-ratio turbofan. The chord length of the blade was 0.25 m, and the cascade was tested at an inlet-to-exit static pressure rise coefficient $C_p = (p_e - p_i)/0.5\rho U_i^2 = 0.45$, which is representative of takeoff loading conditions. The Reynolds number based on chord was maintained above 3×10^5, so the turbulent blade boundary layers and shed wakes are expected to closely approximate those of a full-scale application.[12] More detailed descriptions of the facility have been presented by Waitz et al.[13] and Sell.[14]

Time-mean and unsteady wake velocity measurements downstream from the cascade were taken using a single-element, hot-wire anemometer probe. The error in the velocity measurements was estimated to be less than ±3% with 95% confidence. Wake measurements were taken at downstream locations of 0.5, 1.0, 1.5, and 2.5 chords behind the cascade blades, with the flow traversed parallel to the exit plane of the cascade. Within this region, the static pressure was maintained constant to within ±1.5% of the freestream dynamic head, so that the momentum deficit of the wake was constant to within about 2%.

C. Blowdown Compressor Testing

Wake measurements were also made behind a 0.56-m-diam, 16-blade fan stage. The fan is representative of a next-generation high-bypass application with a tip speed of about M = 0.8, a total pressure ratio of approximately 1.2, a rotor–stator axial spacing of 1.7, and axial velocity variation from rotor to stator of less than 1%. The fan was tested in a tunnel operated in a blowdown manner, as first described by Kerrebrock.[15] The rotor was accelerated to full speed in vacuum and then allowed to spin freely. Then the test was initiated by opening a valve to the supply gas, which allowed the gas to flow through the test section. The rotor speed then decayed as work was done on the flow. The operating pressure in the supply tank was chosen so that, for a period of approximately 100 ms, the decay of the speed of sound of the supply gas was equal to the decay of the rotor speed. In this manner, the rotor was run at constant nondimensional conditions for about 200 rotor flow-through times, over which time the measurements were taken. All measurements were taken at full-speed, takeoff conditions, which are deemed most critical with respect to community noise impact.

The wake measurements were obtained using a four-way probe fitted with four flush-mounted Kulite pressure transducers with vacuum reference, water cooling, and temperature compensation, for measurement of static and total pressure, and two flow angles. A discussion of the design and operating characteristics of this probe is in Ref. 16. Data were taken at a sampling frequency of 333 kHz and low-pass filtered at 50 kHz. The probe was calibrated in a steady flowfield. The flow angles were determined within ±1 deg and the Mach number to within ±2% (except for $z/c < 0.75$, where wake impingement caused oscillations in the probe measurements and reduced the accuracy as will be discussed in Sec. IV.D). Wake measurements were taken at 0.1, 0.5, 1.0, and 1.5 rotor axial chords downstream from the rotor midspan trailing edge. The midspan airfoil and incidence were the same as those used in the cascade experiment described in Sec. III.B. Ensemble-averaging of the wakes was completed over six rotor revolutions to obtain the mean wake profiles, and resolution of turbulent fluctuations was limited to a frequency of about 15 kHz (about seven times blade passing frequency) because of the probe size. Above this frequency, the perturbation wavelength was of the same order, or smaller, than the probe, and thus the perturbation could not be resolved.

D. Navier–Stokes Simulations

In addition to the experimental measurements, computations were undertaken to elucidate the three-dimensional behavior of the wakes shed from the fan geometry described earlier. The NEWT flow solver[16] was used for these calculations. The code uses a multiple-block, unstructured tetrahedral mesh and has provisions for adaptive grid refinement. The three-dimensional, Reynolds-averaged Navier–Stokes equations were solved using a four-step Runge–Kutta time-marching algorithm. Turbulence was simulated using the k-ε model. The code has been used in a variety of other investigations to predict rotor through flow, as well as flow in complex internal blade passages.[17]

The calculation of the fan and downstream flowfield was carried out using 40,000 cells and resulted in an average total pressure rise approximately 1% lower than that measured in the rig tests. The pressure rise and turning were within 1% at the 75% span location, which was chosen for comparison with the rig test results and the simplified model. However, approximately 5% less total pressure rise was apparent at the 50% span location in the calculation than at the same location in the experiment. In addition, the calculated wakes were deeper and narrower than those measured experimentally, indicating that the grid was not sufficiently resolved and/or that the turbulent viscosity was not being accurately represented. Nonetheless, the calculations were useful for illustrating the effects of skew in a situation more complex than could be represented using the simplified two-dimensional model.

IV. Results and Discussion

In Sec. IV.A, the simplified numerical model is compared to measurements taken in the cascade facility. The effects of skewing and stretching of the wake on the wake velocity deficit and width are then parameterized in Sec. IV.B. Section IV.C presents the comparison of the model to the three-dimensional computations, and in Sec. IV.D, estimates from the model are compared to measurements obtained from the fan rig. A brief discussion of implications for the design of turbomachine blades so that the wakes decay more rapidly is given in Sec. IV.E.

A. Validation of the Simplified Numerical Model with Two-Dimensional Cascade Data

The numerical scheme used to integrate Eqs. (9) was first validated by comparing the results of the simplified numerical model to an exact error function solution for a double-diffusion layer problem. The computed diffusion layer profile matched the analytical solution with less than 1% error. Following this, the model was compared to cascade wake measurements. For two-dimensional wakes, the turbulent viscosity is approximately constant with downstream distance.[18] Therefore, a constant effective viscosity of 0.0275 m^2/s was chosen for these comparisons. This value of viscosity provided the best match between the modeled and measured two-dimensional wake decay rates. The calculations were initiated using a Gaussian velocity profile that was specified to approximate the measured wake profile at 0.5 chords downstream. The calculated velocity profiles at 0.5, 1.0, 1.5, and 2.5 chords are compared to the measured cascade profiles in Fig. 4. For this two-dimensional case with no stretching, both the velocity deficit and width are accurately captured by the model. The calculated velocity deficit is within 5% of the measured values at 1.5 and 2.5 chords.

B. Effect of Wake Skew

We begin with a qualitative discussion of the effect of stretching on wake mixing and then use the simplified model to quantitatively parameterize the effects. Stretching of the vorticity associated with the wake tends to increase the strength of the vorticity and thus the gradients in $w(y)$. At the same time, the induced normal velocity v_s moves the shear layers closer together. This effectively results in more rapid mixing and an increase in the wake centerline velocity, but also smaller wake width in the y direction than with no stretching. Thus, the momentum thickness of the wake measured normal to the wake centerline is smaller with stretching applied. However, because the stretching is a result of wake skewing, the wake is oriented at some angle relative to the radial direction (as shown in Fig. 1). Thus, when the velocity deficit is measured in the circumferential direction, i.e., at the skew angle ζ through the model wake, the width is increased over the unstretched wake. This results in constant wake momentum thickness downstream (when measured in the circumferential direction) with the decrease in velocity deficit, as required for

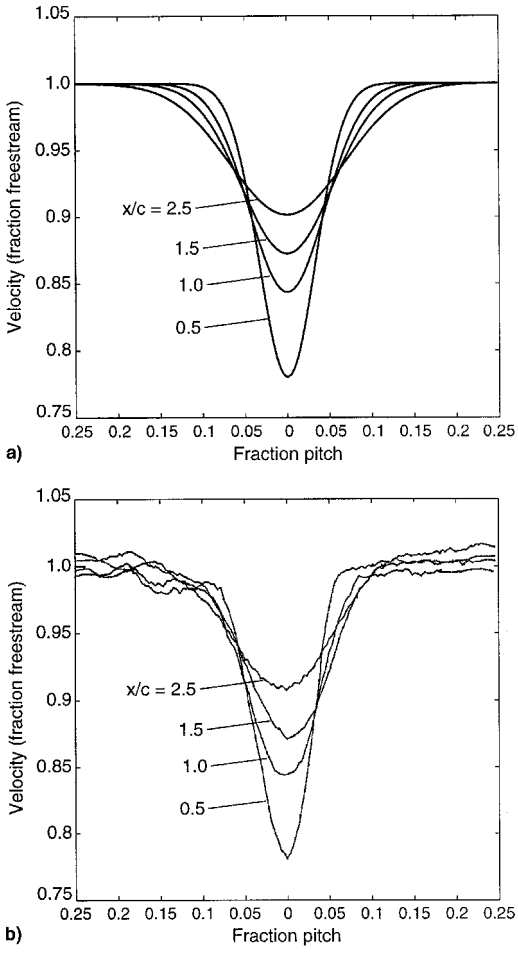

Fig. 4 Comparison of a) simplified numerical model and b) cascade wake data (no skew or stretching).

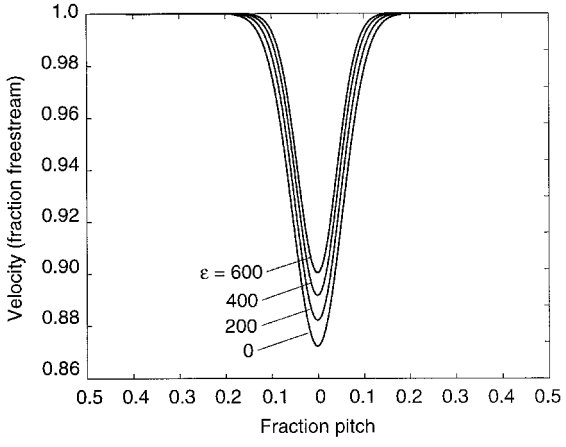

Fig. 5 Model calculations—effect of stretching on the wake profile at 1.5 chords (wake relative coordinates).

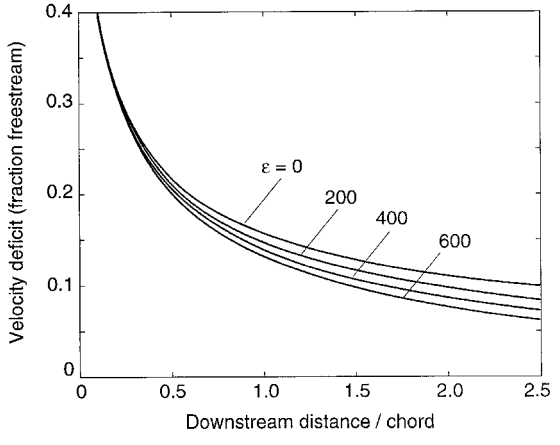

Fig. 6 Model calculations—effect of stretching on the wake velocity deficit.

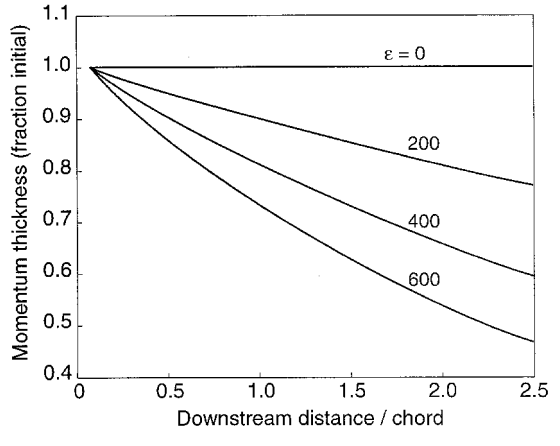

Fig. 7 Model calculation—effect of stretching on the wake momentum thickness (wake relative reference frame).

momentum conservation under conditions of zero axial pressure gradient and no spanwise transport of wake fluid.

The effects of stretching on wake mixing will now be examined quantitatively using the simplified model. Different strain rates were applied to the wake to determine the parametric trends for wake velocity deficit and width. The initial conditions and effective viscosity obtained from the comparison to the cascade measurements were used for the investigation. Constant strain rates downstream from the rotor ranging from $\varepsilon = 0$ to 600 were specified. These strain rates cover the range of interest for typical turbomachine applications.

Figure 5 shows the wake velocity profiles in the wake relative frame at 1.5 chords downstream for the different strain rates examined. The reduction in both the velocity deficit and width of the wake with increased strain rate is shown. The reductions in deficit and width increase with downstream distance because the wake is stretched to ever-increasing length. The decay of the centerline velocity deficit with downstream distance is plotted in Fig. 6 for the different strain rates. There is rapid decay of the velocity deficit in the near-wake region (up to about 0.5 chords). The decay rate then decreases with downstream distance. For a typical fan rotor–stator spacing of approximately 1.5 chords and a strain rate of 600 (which would roughly correspond to the local strain rate near the hub for a rotor designed for constant radial work input with a hub-to-tip ratio of 0.5), the wake at the stator position will have a velocity deficit of about 78% of that which would be predicted with an unstretched cascade wake. For prediction of unsteady loading on the stator blade and radiated noise, this would result in an error of approximately 2 dB. A more detailed discussion of the effect of wake skew and stretch on wake harmonic amplitudes, and thus the effect on radiated tonal noise, is presented in Sec. IV.E.

As discussed previously, the wake momentum deficit measured normal to the wake (the y direction in the wake relative frame) decays with downstream distance as the wake is stretched. A plot of this decay is presented in Fig. 7. For the example given earlier of a constant radial work fan with a hub-to-tip ratio of 0.5, the momentum thickness is decreased by approximately 37% compared to the unstretched case at 1.5 chords downstream from the rotor. This decay in the momentum thickness is related to the wake skew angle by $\theta/\theta(0) =$

cos ζ. When the momentum thickness is measured circumferentially in the absolute frame, the momentum thickness is constant with downstream distance.

C. Comparison with Navier–Stokes Simulations for a High-Speed Fan Rotor

Rotors typically have radial gradients in both axial and tangential velocity resulting in a radial variation of the wake skew angle and, thus, spatial variations in the strain rate applied to the wake. Also, strong radial wake transport is often observed. To investigate the effects of stretching on wake mixing in a situation that is more representative of a fan application, the wake velocity profiles obtained from the simplified numerical model were compared to the results of three-dimensional computations. The appropriate strain rates were obtained by plotting contours of relative Mach number to determine the skew angle of the wake at 0.1, 0.5, 1.0, and 1.5 chords downstream. These plots are shown in Fig. 8. Seventy-five percent span was chosen for the comparison because it is a region of high wake stretching, and this spanwise location is outside the tip clearance flow region. Further, because there is approximately zero radial gradient in axial velocity at 75% span, the angle of intersection of the wake with an axial plane as shown plotted in Fig. 8 corresponds approximately to the angle of the projection of a wake vortex line onto that plane. (Recall that the projection is the relevant angle for determining wake stretching caused by swirl, as discussed in Sec. II.B.2.) A Gaussian profile that approximates the computational wake profile at 0.1 chords was used for the initial condition, and the effective viscosity, $\nu = 0.040$ m^2/s, was set in the simplified model to match the change in the computational wake profile between 0.1 and 0.5 chords. This is an acceptable procedure for setting the effective viscosity because there is negligible wake stretching between the trailing edge and 0.5 chords downstream. (Indeed, the effect of wake stretching on velocity deficit in this region is less than 2%.) A comparison of the wake profile from the three-dimensional simulation, the unstretched model wake, and the stretched model wake at 0.5 chords is shown in Fig. 9b. The model wake captures the overall features of the wake obtained from the three-dimensional simulation.

The wake velocity profiles at 1.0 and 1.5 chords downstream are compared to the results of the three-dimensional computations in Figs. 9c and 9d. The strain rates specified in the simplified model were estimated from the wake skew angles calculated from the Navier–Stokes solver. The predicted wake velocity deficits compare within 3.5%. Also plotted are the wake profiles that would result if no stretching were introduced into the simplified model. The reduction in wake velocity deficit caused by stretching corresponds to approximately 12% of the unstretched deficit at 1.5 chords downstream from the blade.

D. Comparison with Fan Wake Measurements

In this section the results of the simplified calculation procedure are compared to measurements behind a rotating blade row. To accomplish this, measured wake data immediately downstream from the blade row were used to set the initial wake profile for the computation, and the change in measured wake profiles between 0.1 and 0.5 chords was used to set the effective viscosity. This is the same procedure that was used for the comparison to the Navier–Stokes solution presented in Sec. IV.C. Wake measurements at 1.0 and 1.5 chords downstream were then compared to the simplified model with and without strain imposed.

The wake initial condition was established by matching the momentum deficit measured downstream from the fan and the measured wake velocity profile at 0.1 chords to within 3% of velocity deficit and 32% of the width. Because the wake at 0.1 chords was relatively small compared to the four-way probe, the measurements were less accurate at this location. Further,

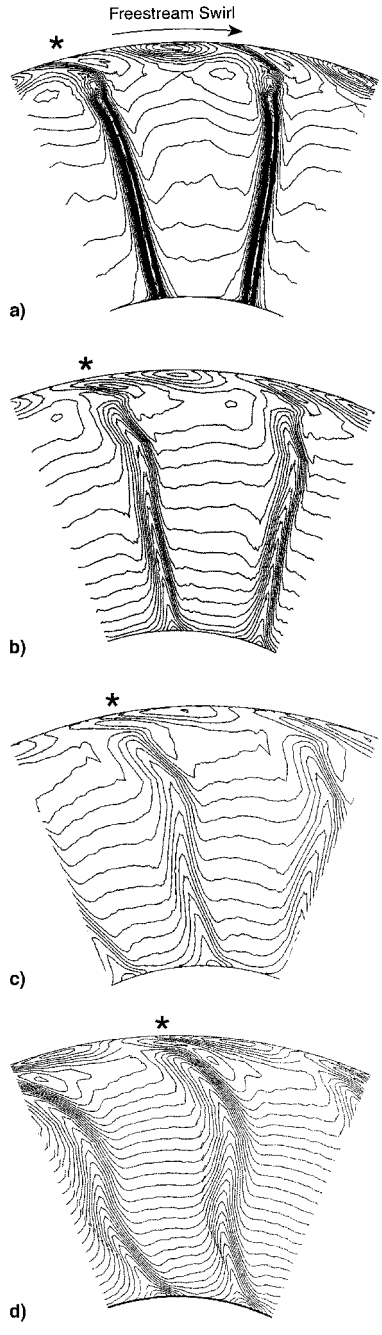

Fig. 8 Fan wake behavior: Mach number contours from three-dimensional Navier–Stokes simulation. Blade rotation is clockwise at about twice the speed of the tangential wake convection (* denotes a particular wake). x/c = a) 0.1, b) 0.5, c) 1.0, and d) 1.5.

oscillations in measured flow Mach number were observed that are believed to have resulted from amplification of unsteady vortex shedding on the probe because of the wake impingement. These oscillations (which can be seen in Figs. 10a and 10b) are thus an artifact of the measurement device and were not present in the flow. It was found, however, that the initial condition used at 0.1 chords had little impact on the comparison between calculated and measured wake characteristics, provided the momentum thickness of the model wake at 0.1 chords was set to match that measured downstream. The effective viscosity was set to obtain the measured velocity deficit at 0.5 chords, resulting in $\nu = 0.044$ m^2/s. As discussed in Sec. III.A, the difference between this viscosity and that required to match the results of the cascade experiments scales roughly

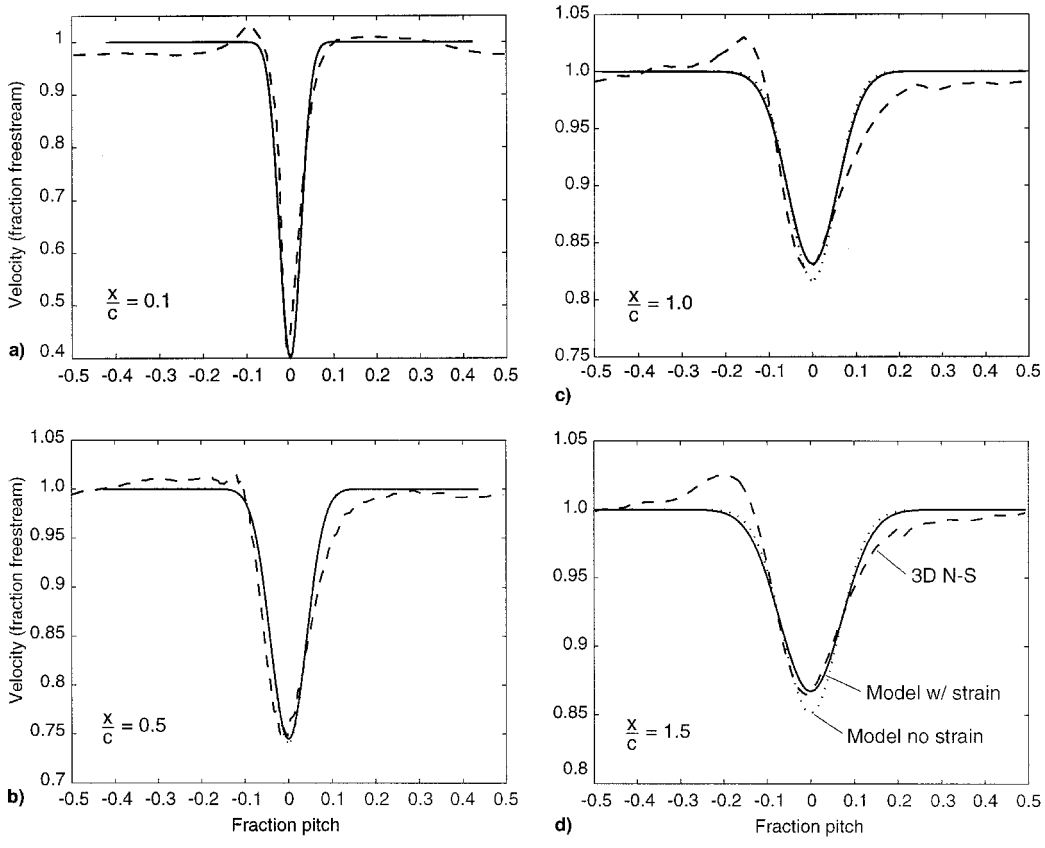

Fig. 9 Comparison of results from simplified numerical model and three-dimensional Navier–Stokes simulation. (Note that Figs. 9a–9d are plotted on different scales.)

with the increase in mean shear because of the additional radial transport velocity measured in the rig tests. Therefore, setting the model viscosity in this manner may approximately capture the increased turbulent exchange associated with radial wake transport.

Wake measurements taken at 50 and 75% span in the experiment were used with a rotor shaft speed encoder signal to estimate the tangential position of the wakes. The wake unsteadiness and variability made it difficult to discern the center of the wake in raw data traces to better than 2% pitch, and a more detailed mapping of the wake position as a function of radius was not possible at the time. However, the measurements taken at 50 and 75% span indicate that the wake was more highly skewed in the outer one-half span than the results of the three-dimensional computations presented in Sec. IV.C suggest. The measured data show the 75% span wake to be shifted an additional 10% in pitch from the calculation relative to the 50% span wake location at 1.5 chords. This is caused by a slightly different loading distribution in the Navier–Stokes solver as discussed in Sec. III.D. With the loading shifted relatively further outboard on the blade in the simulations, the simulated skew angle is lower than that measured in the experiment. The wake skew angle in the rig test was approximately 55 deg at 1.5 chords and 75% span.

The strain rates corresponding to the wake skew angles measured in the data were specified in the simplified numerical model. The results are compared to the measured wake velocity profiles in Figs. 10a–10d. As in Sec. IV.C, all of the wake comparisons were carried out for the 75% span location. Addition of stretching to the model accounts for 73% of the difference between two-dimensional wake evolution and the wake decay in the flowfield downstream from the rotating fan. The additional differences between the estimated wake and the measured wake may be a result of the experimental uncertainty and/or redistribution of wake fluid caused by radial transport. Nonetheless, the results imply that wake stretching has a significant effect on the behavior of the wake.

E. Wake Stretching Effects on Radiated Acoustics

The effects of wake skewing on the coupling of the wake–stator interaction to the duct acoustic modes are relatively well known. These effects are a result of the radial variation in time at which the wake intersects the stator leading edge, and changes in this distribution can either increase or decrease the resulting acoustic amplitudes. In addition to these changes, however, the effect of skewing on the mixing rate of the wake can further affect the radiated noise. To examine these latter effects, the modeled wakes at 1.5 chords for the stretched and unstretched cases were spatially decomposed into harmonics of blade passing frequency (BPF). The resulting harmonic amplitudes for the two cases are plotted in Fig. 11. These are compared to the harmonic amplitudes obtained from the wakes measured in the fan rig tests. Because the amplitudes of radiated acoustic modes associated with wake–stator interaction vary approximately linearly with the amplitudes of the wake harmonics impinging on the stator blades, reductions in acoustic levels can be estimated from reductions in the wake harmonics. The reductions are given by $\Delta dB = 20 \log_{10}(A_{st}/A)$, where A is the harmonic amplitude of the unstretched wake, and A_{st} is the harmonic amplitude of the stretched wake. Stretching of the wakes results in noise reductions of about 2.5 dB for the 2 × BPF mode and more than 5 dB for the higher harmonics.

These reductions imply that fan loading could be tailored to produce perhaps 3-dB reductions in radiated tonal noise above present designs. [It is also expected that wake stretching will have some impact on the turbulent fluctuations in the wake that give rise to broadband noise. Studies of wakes downstream from wings presented by Miranda and Devenport[19] generally showed large increases in turbulence levels in regions

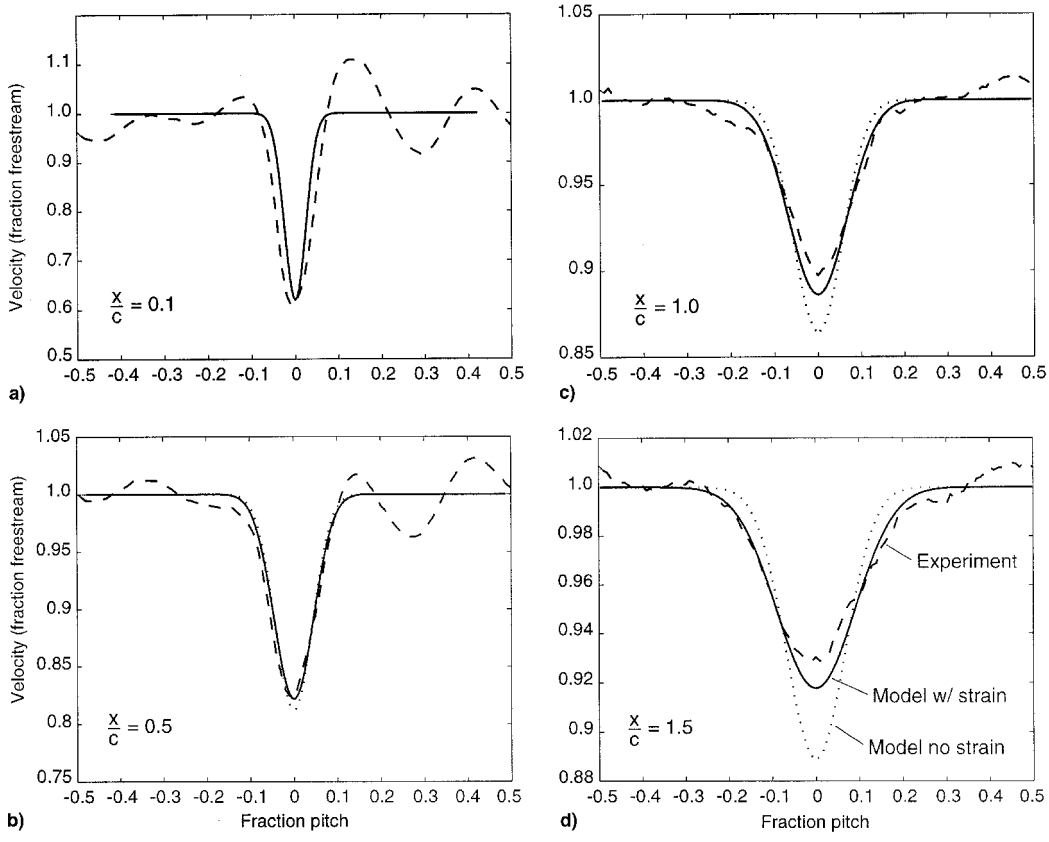

Fig. 10 Comparison of results from simplified numerical model and fan rig measurements. (Note that Figs. 10a–10d are plotted on different scales.)

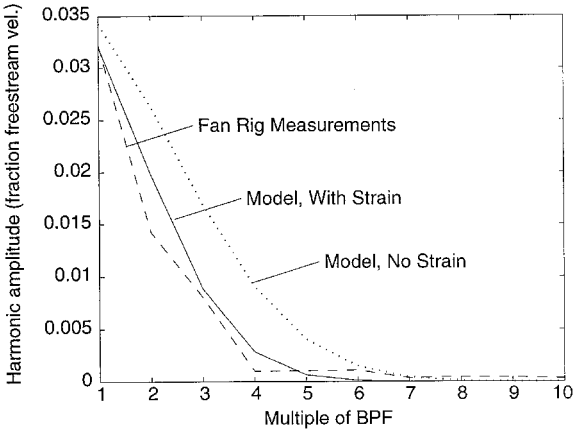

Fig. 11 Spatial harmonic content of wake profiles at 1.5 chords.

of the wake undergoing straining when the turbulent stresses are normalized by the local length and velocity scales. However, the absolute (dimensional) magnitudes of the turbulent stresses changed little with increased strain rate.] If studies are conducted to determine the most dominant spanwise sections of the stator with respect to coupling with the propagating acoustic modes, then the blade loading can be designed to give the greatest stretching in that region. This would be done through designing the blades to give appropriate radial gradients in the tangential and axial velocities. The reductions associated with more rapid wake decay must be considered with respect to additional changes (either increases or decreases) in radiated noise because of the variation in coupling to duct modes as the wakes are skewed relative to the stator blades. Further, design changes to achieve noise reductions must be balanced against efficiency and performance issues to determine the best overall design.

IV. Summary and Conclusions

A simplified numerical model was developed to quantitatively describe the effects of swirl on the decay of wakes downstream from rotating blade rows. Freestream swirl skews the wake tangentially and stretches the wake as it is convected downstream. These effects cause the velocity deficit to be reduced and the width of the wake measured in the circumferential direction to be increased. Wake skewing has little impact on wake decay when rotor–stator axial spacing is less than 40% chord, and/or the hub-to-tip ratio is over 0.9. However, for low hub-to-tip ratio machines with large rotor–stator spacing, typical of fans in high-bypass-ratio turbomachines, stretching of the wake and the associated effects on the wake decay characteristics can be large. In such situations, 50% reduction in the wake velocity deficit is possible.

Cascade wake profiles were estimated to within 5% of the velocity deficit by the simplified numerical model with no stretching. With the introduction of stretching into the model, the wake velocity deficit downstream of a next-generation high-bypass-ratio turbofan was estimated to within 13%. It was shown that the change in wake decay with stretching may be responsible for between 2.5 and 5 dB changes in radiated tone noise.

Use of constant effective viscosity and constant average strain rate was seen to adequately capture the essential physics of the wake mixing behavior.

Finally, this study suggests that the use of cascade data and two-dimensional wake mixing models for the prediction of unsteady aerodynamics and noise associated with wakes interacting with downstream blade rows must be done with care. However, the application of wake stretching to simplified mod-

els of wake mixing can be used to extend the range of applicability of two-dimensional cascade data.

Acknowledgments

This work was supported by NASA Grant NAG1-1512. We thank Pratt and Whitney for providing the fan geometry used in this study. D. B. Hanson and K. U. Ingard provided many insights into turbomachine noise, and N. A. Cumpsty and A. H. Epstein taught us about several aspects of fan flowfields. We also thank W. N. Dawes for help in using the Navier–Stokes solver. In addition, the technical support of V. Dubrowski is greatly appreciated. Finally, we thank the Technical Monitor, C. H. Gerhold, and D. G. Stephens, both of NASA Langley Research Center, for their continued interest and support.

References

[1]Epstein, A. H., Gertz, J. B., Owen, P. R., and Giles, M. B., "Vortex Shedding in High-Speed Compressor Blade Wakes," *Journal of Propulsion and Power*, Vol. 4, No. 3, 1988, pp. 236–244.

[2]Ng, W. G., and Epstein, A. H., "Unsteady Losses in Transonic Compressors," *Journal of Engineering for Power*, Vol. 107, April 1985, pp. 345–353.

[3]Lakshminarayana, B., Govindan, T. R., and Reynolds, B., "Effects of Rotation and Blade Incidence on the Properties of the Turbomachinery Rotor Wake," AIAA Paper 81-0054, Jan. 1981.

[4]Prato, J., and Lakshminarayana, B., "Investigation of Compressor Rotor Wake Structure at Peak Pressure Rise Coefficient and Effects of Loading," *Journal of Turbomachinery*, Vol. 115, July 1993, pp. 487–500.

[5]Suryavamshi, N., and Lakshminarayana, B., "Numerical Prediction of Wakes in Cascades and Compressor Rotors Including the Effects of Mixing, Part II," American Society of Mechanical Engineers, Paper 91-GT-222, June 1991.

[6]Hanson, D. B., "Coupled Two-Dimensional Cascade Theory for Noise and Unsteady Aerodynamics of Blade Row Interaction in Turbofans," NACA CR-4506, Jan. 1994.

[7]Philbrick, D. A., and Topol, D. A., "Development of a Fan Noise Design System. Part I: System Design and Source Modeling," AIAA Paper 93-4415, Oct. 1993.

[8]Kerrebrock, J. L., *Aircraft Engines and Gas Turbines*, 2nd ed., MIT Press, Cambridge, MA, 1992.

[9]Papamoschou, D., and Roshko, A., "The Compressible Turbulent Shear Layer: An Experimental Study," *Journal of Fluid Mechanics*, Vol. 197, Dec. 1988, pp. 453–477.

[10]Waitz, I. A., Elliot, J. K., Fung, A. K. S., Kerwin, J. M., Krasnodebski, J. K., O'Sullivan, M. N., Qui, Y. J., Tew, D. E., Greitzer, E. M., Marble, F. E., Tan, C. S., and Tillman, T. G., "Streamwise-Vorticity-Enhanced Mixing," *Progress in Aerospace Sciences*, Vol. 33, No. 5, 6, 1997, pp. 323–352.

[11]Hill, P. G., Schaub, U. W., and Senoo, Y., "Turbulent Wakes in Pressure Gradients," *Journal of Applied Mechanics*, Dec. 1963, pp. 518–524.

[12]Cumpsty, N. A., *Compressor Aerodynamics*, Wiley, New York, 1989.

[13]Waitz, I. A., Brookfield, J. M., Sell, J., and Hayden, B. J., "Preliminary Assessment of Wake Management Strategies for Reduction of Turbomachinery Fan Noise," *Journal of Propulsion and Power*, Vol. 12, No. 5, 1996, pp. 958–966.

[14]Sell, J., "Cascade Testing to Assess the Effectiveness of Mass Addition/Removal Wake Management Strategies for Reduction of Rotor-Stator Interaction Noise," M.S. Thesis, Dept. of Aeronautics and Astronautics, Massachusetts Inst. of Technology, Cambridge, MA, 1997.

[15]Kerrebrock, J. L., "The MIT Blowdown Compressor Facility," MIT Gas Turbine Lab Rept. 108, Cambridge, MA, 1972.

[16]Reijnen, D., "An Experimental Study of Boundary Layer Suction in a Transonic Compressor," Ph.D. Dissertation, Dept. of Aeronautics and Astronautics, Massachusetts Inst. of Technology, Cambridge, MA, 1997.

[17]Dawes, W. N., "The Practical Application of Solution-Adaption to the Numerical Simulation of Complex Turbomachinery Problems," *Progress in Aerospace Sciences*, Vol. 29, No. 3, 1992, pp. 221–269.

[18]Schlichting, H., *Boundary Layer Theory*, McGraw–Hill, New York, 1979.

[19]Miranda, J. A., and Devenport, W. J., "Two-Point Measurements in Trailing Vortices," AIAA Paper 96-0804, Jan. 1996.